

PACS numbers: 73.61.Ey, 75.70. – i, 85.40.Ls

**MAGNETIC, ELECTRICAL AND SURFACE MORPHOLOGICAL
CHARACTERIZATION OF AuGe/Ni/Au OHMIC CONTACT
METALLIZATION ON GaAs/AlGaAs MULTILAYER STRUCTURES**

T.S. Abhilash, Ch. Ravi Kumar, G. Rajaram

School of Physics and Centre for Nanotechnology,
University of Hyderabad, Hyderabad – 500046, India
E-mail: abhilashthanniyil@gmail.com

A process issue arising from the use of ferromagnetic Nickel in the AuGe/Ni/Au Ohmic contact metallization is studied in the context of magnetic field sensors and HEMT devices made using GaAs/AlGaAs multilayer structures with the two dimensional electron gas layer. The dependence of magnetization, contact resistance, adhesion, surface roughness and current distribution of alloyed Ohmic contacts on parameters such as Ni layer thickness, anneal temperature and Au-Ge alloy composition are discussed. The magnetization measurements provided some new and interesting insights into changes occurring in the metallization layers prior to alloying.

Keywords: GaAs/AlGaAs, HALL SENSORS, MAGNETIC PROPERTIES, OHMIC CONTACT.

(Received 04 February 2011, in final form 28 April 2011)

1. INTRODUCTION

GaAs/AlGaAs multilayer structures, incorporating the 2-dimensional electron gas (2 DEG) layer, are useful for the fabrication of High Electron Mobility Transistors (HEMTs) and Hall Effect based magnetic field sensors [1, 2]. A popular recipe for fabricating Ohmic contacts to these structures is the deposition of a metallization structure with eutectic AuGe (88:12 wt %)/Ni/Au, followed by rapid thermal alloying [3-5]. This recipe gives low contact resistance with moderate surface roughness which can be further improved by increasing Ni layer thickness or decreasing the Ge content below that of the eutectic composition (88:12 wt %), at the expense of increase in contact resistance [6-9]. The use of Ni, however, could render the structure magnetic and may cause perturbation of the measured field in Hall magnetic field sensors.

Despite the use of AuGe/Ni/Au Ohmic contacts to GaAs/AlGaAs for quite some time, systematic magnetic data of the contact structure are scarce in the literature. Sensor fabricators tend to use alternatives such as Cr, Ti etc. as the interlayer. However these formulations produce a rougher morphology after processing. The Ni based contacts are popularly used in HEMTs where lateral roughness of the contacts near the gate needs to be minimized. Therefore, in the context of Hall magnetic field sensors with on-chip circuits, a process optimization needs to be carried out, wherein all three parameters- magnetization, contact resistance and roughness are considered. This paper reports magnetization, contact resistance, topography and current distribution data, in samples with varying AuGe compositions

and Ni-layer thicknesses. The magnetization measurements have provided some interesting insights into changes that occur in the metallization layer prior to alloying and are discussed.

2. EXPERIMENTAL DETAILS

The GaAs/AlGaAs multilayer structure used in this study is grown by Molecular Beam Epitaxy (MBE). The contact metallization structure used is given in table 1.

Table 1 – Ohmic contact metallization

Au (200 nm)
Ni (10 ÷ 100 nm)
Eutectic/off – eutectic AuGe (100 nm)
GaAs/AlGaAs multilayer wafer with n ⁺ GaAs cap layer

Metallizations with three AuGe compositions - eutectic (88:12 wt %) and off-eutectics (95:5 and 97.3:2.7 wt %) – were investigated. The contact resistances were measured by lithographically patterning a transmission line pattern as described in [9] and using the Transmission line or Transfer Length Model (TLM) [10]. The metallization structure was prepared by evaporating AuGe (100 nm), Ni (10, 25, 30, 50, 75, 100 nm) and Au (200 nm) using thermal, e – beam and thermal evaporation respectively. The samples were subjected to anneals at temperature T_A , reached at heating rates of 250 °C/min, held at T_A for durations, t_A (typically 1 minute), and then cooled down followed by magnetic hysteresis loop measurements at room temperature using a Vibrating Sample Magnetometer (VSM).

The surface roughness was estimated by measuring the root-mean-square height of the sample over an area of about 5 $\mu\text{m} \times 5 \mu\text{m}$, at several pads of the TLM structure using Atomic Force Microscopy (AFM). Temperature scans of Differential Scanning Calorimetry (DSC) were performed on the metallized substrate, from room temperature to 500 °C at a heating rate of 100 °C/min. The current distribution over the alloyed pads was imaged using a conducting probe-AFM (CAFM) in contact mode on the surface of samples with eutectic-AuGe/Ni/Au metallization and that gave the optimum contact resistance.

3. RESULTS AND DISCUSSIONS

Some of the non-magnetic alternatives to Ni used by sensor fabricators are Cr, Ti, Pd, Pt etc. [11]. In this study, a comparison of the contact resistance and surface roughness were carried out as the interlayer is changed from Ti to Cr to Ni. It is seen that the surface roughness decreases as the interlayer is varied from Ti to Ni. Fig. 1 shows SEM micrographs of the alloyed contacts with Ti and Ni as the interlayer.

Fig. 2 shows contact resistance vs. anneal temperature for Ohmic contact metallization structures with Ti, Cr, Ni and no interlayer between AuGe and Au layers. Clearly, metallization with Ni interlayer is the best choice in terms of contact resistance and surface roughness. Hence an optimization of the Ni layer thickness is necessary, in order to reduce contact resistance and surface roughness.

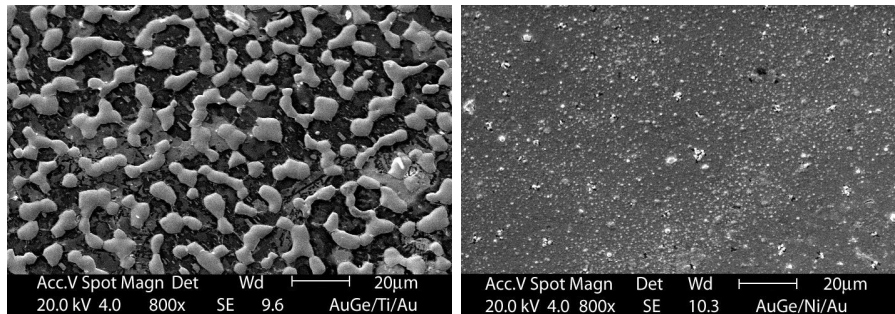


Fig. 1 – SEM micrographs of the surface of AuGe/Ti/Au and AuGe/Ni/Au contact metallization structures, annealed at 400 °C

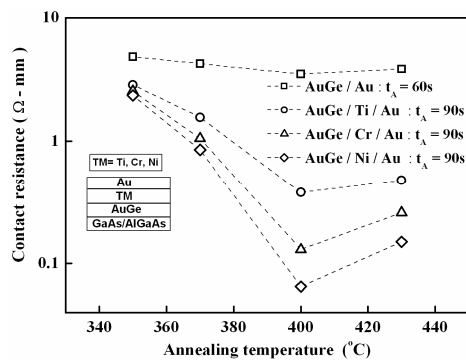


Fig. 2 – Contact resistance as a function of anneal temperature for AuGe/TM/Au. TM = Ti, Cr and Ni or none. The lines are a guide to the eye

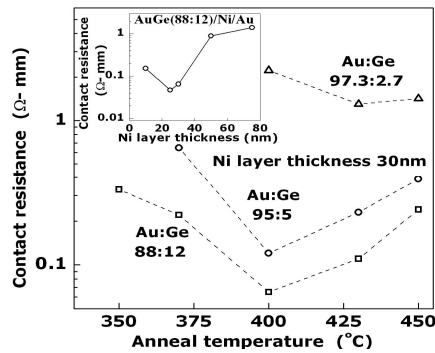


Fig. 3 – Contact resistance Vs anneal temperature for different AuGe compositions and Ni layer thicknesses

The Optimization of Ni layer thickness for reduced contact resistance and surface roughness was carried out. The contact resistances for different Ni-layer thickness on samples with fixed eutectic AuGe layer thickness of 100 nm indicate that the lowest contact resistance of $0.05 \pm 0.01 \Omega\text{-mm}$ is obtained at a Ni layer thickness of 25 nm (inset of Fig. 3) [9]. Increasing the

Ni layer thickness or decreasing the Ge content from the eutectic composition increases the contact resistance but decreases surface roughness (table 2). Increasing Ni layer thickness (50 nm) above the optimum decreases roughness by 50 % but increases contact resistance by a factor of ~ 10. On the other hand, use of the off-eutectic alloy with 95:5 wt % results in reduction of surface roughness by 75 % whereas contact resistance increases only by a factor of 2 over that for eutectic composition as shown in Fig. 3. Clearly, use of off-eutectic AuGe (95:5) alloy with optimum Ni layer thickness appears to be a good choice in trading off contact resistance for surface roughness than increasing Ni layer thickness above the optimum using the eutectic alloy (Fig. 3) [12].

Table 2 – Contact resistance, surface roughness and anneal temperature required to complete magnetic to non-magnetic transition for different AuGe compositions and Ni layer thicknesses

AuGe alloy composition (wt %)	Ni layer thickness, (nm)	Contact resistance (Ω -mm)	Surface roughness (nm)	Magnetic to non-magnetic transformation temperature ($^{\circ}$ C)
88 : 12	10	0.15	25 ± 4	100 – 200
88 : 12	25	0.05 ± 0.01	21 ± 3	200 – 250
88 : 12	50	0.90	11 ± 1	250 – 300
88 : 12	75	1.40	7.5 ± 0.5	350 – 400
95 : 5	30	0.17 ± 0.02	5.5 ± 0.5	250 – 300
97.3 : 2.7	30	1.30	4.5 ± 0.5	400 – 430

The room temperature magnetization of samples annealed at various anneal temperatures, is shown in Fig. 4, as a percentage of the magnetization of the un-annealed sample.

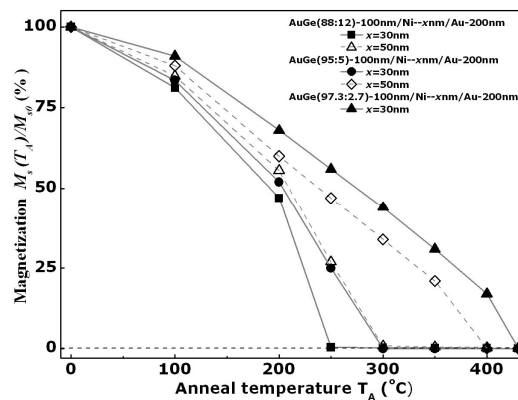


Fig. 4 – Decrease in magnetization upon annealing, for contact metallization structures with three AuGe alloy compositions and different Ni layer thicknesses

The as-deposited film structures are ferromagnetic. The magnetization progressively decreases to zero as the anneal temperature is increased. The magnetization studies indicate that the conversion of Ni to non-magnetic phase

begins at anneal temperatures as low as 100 °C and the structure becomes completely non-magnetic at room temperature after annealing at 400-430 °C with different Ni layer thickness and Ge content in the AuGe alloy (Table 2).

The magnetic measurements, apart from confirming that the contacts prepared by the conventional recipe are indeed non-magnetic, provide additional insights into changes taking place in the metallization structure before alloying occurs. Data for metallizations with varying AuGe layer thicknesses show that the fraction of Ni converted to non-magnetic phase is the same for all samples with the same Ni/AuGe layer thickness ratio. This dependence on the AuGe layer thickness implies that the entire AuGe layer, and not just the interface, participates in this conversion of Ni layer to a non-magnetic phase, which is not only partial for low temperature anneals, but is time independent. The observation that the fraction of Ni converted to non-magnetic form scales with AuGe layer thickness-shows that the transformation of the Ni layer to a non-magnetic phase occurs through dissolution into the AuGe layer.

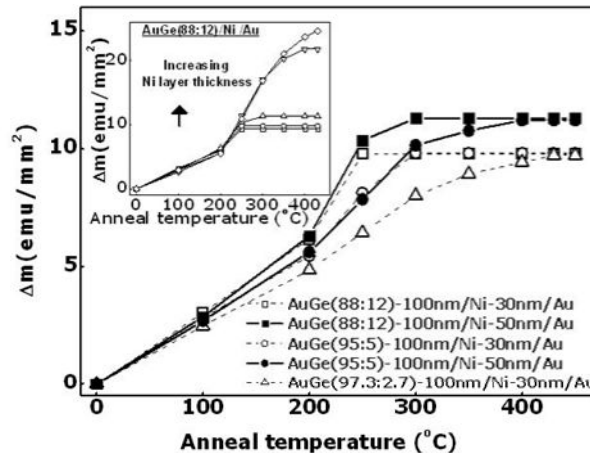


Fig. 5 – Effective thickness of Ni layer transformed to non-magnetic phase on annealing at various temperatures. (Δm is the decrease in magnetization per unit area)

This dissolution is solubility limited, with the solubility varying with temperature. This is demonstrated in Fig. 5. It is seen that a quantity proportional to the Ni-layer thickness transformed to the non-magnetic phase increases with anneal temperature and is independent of initial Ni layer thickness until all the Ni is transformed. Fig. 5 also demonstrates that, when the Ge content in AuGe is decreased, the solubility for Ni decreases.

Two distinct layers (Fig. 6) are observed (Au over-layer and AuGe(Ni) layer) in cross sectional SEM after Ni is completely converted and just before alloying, implying that the transformation of Ni to non magnetic phase occurs in the solid state [10,12,13].

Grazing incident XRD data indicate the presence of Ni – Ge phases in the structure when the magnetic to non-magnetic transformation takes place after annealing at 300 °C and cooled down to room temperature. TEM [14-17] studies also indicate the presence of Ni₃Ge ($T_A \sim 400$ °C) after anneals



Fig. 6 – Cross sectional SEM of AuGe (88 : 12 wt %) - 100 nm / Ni - 25 nm / Au - 200 nm annealed at 300 °C and cooled down to room temperature

at temperatures close to the alloying temperature. A picture consistent with this data is that Ni dissolves into AuGe in a solid state solubility limited process and precipitates as NiGe compounds on cooling down to room temperature. The formation of these NiGe compounds reduces availability of Ge for alloying, leading to an optimum Ni layer thickness for best contact resistance.

Alloying between the metallization structure and the substrate seems to occur for $T_A > \sim 400$ °C and when melting takes place in the metallization structure. Signatures of melting (endothermic peaks correlating well with roughness increases) are detected in Differential Scanning Calorimetry (DSC) scans (Fig. 7).

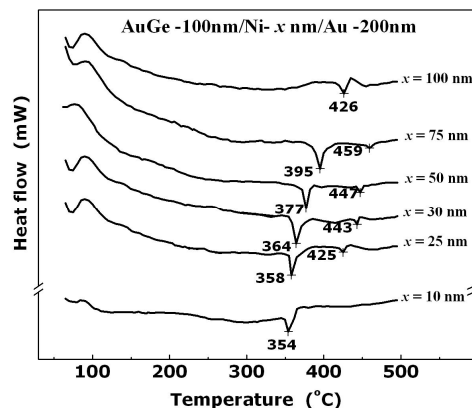


Fig. 7 – DSC scans for samples with metallization structures with eutectic AuGe (88 : 12) alloy layer and different Ni layer thicknesses

The melting temperature of the metallization structure increases with increase in Ni layer thickness (increased Ni concentration in AuGe before melting) as well as with decrease in Ge content, consistent with in-situ XRD studies [18]. It is likely that the surface roughness reductions obtained by varying these process parameters are related to this melting. The adhesion of the metallization structure with the underlying substrate (observed using Nano-indenter scratch tests) also improves with increasing Ni layer thickness. Both these effects contribute to better contact area and thus contact resistance and smoothness.

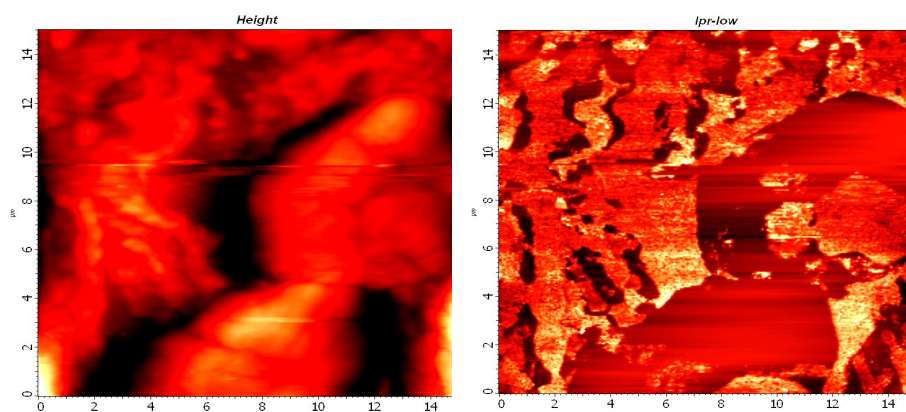


Fig. 8 – Surface topography and current mapping of AuGe/Ni/Au which shows the least contact resistance

The topography and current distribution of annealed AuGe/Ni/Au contacts, with varying Ni layer thicknesses, were studied by CAFM. The topography and current images obtained simultaneously at a bias voltage of 8 V for AuGe/Ni (25 nm)/Au are shown in Fig. 8. The topographic and current images show a uniform surface for Ni layer thickness of 100 nm as well as for all as-deposited un-annealed metallization structures. Samples with optimized contact resistance show spatially non-uniform current distribution. The images in Fig. 8 indicate short distance current fluctuations as well as fluctuations correlated with micron-sized surface features. Clearly, the integrity of the Au over-layer is severely affected during the melting/alloying process.

4. CONCLUSIONS

The metallization structures are rendered non-magnetic at room temperature after annealing at typically used alloying conditions. The magnetic measurements are suggestive of solid state solubility limited dissolution of Ni into AuGe followed by segregation into non magnetic Ni – Ge compounds. The optimum contact resistance of $\sim (0.05 \pm 0.01 \Omega \cdot \text{mm})$ is obtained at a Ni layer thickness of 25-30 nm for 100 nm AuGe layer thickness. The surface roughness decreases, metallization melting temperature increases and the adhesion improves on decreasing Ge content in the alloy or with increasing the Ni layer thickness. The current distribution is non-uniform with short and long range fluctuations.

The authors acknowledge the support of UGC (UPE, CAS programmes), ACRHEM, BRNS / IGCAR and DST (Centre for Nanotechnology).

REFERENCES

1. J.W. Lim, H.K. Ahn, H.G. Ji, W.J. Chang, J.K.Y. Mun, H. Kim, *Semicond. Sci. Tech.* **19**, 1416 (2004).
2. Y. Sugiyama, *J. Vac. Sci. Technol. B* **13**, 1075 (1995).
3. M. Murakami, *Sci. Technol. Adv. Mat.* **3**, 1 (2002).

4. R.P. Taylor, P.T. Coleridge, M. Davies, Y. Feng, J.P. McCaffrey, P.A. Marshall, *J. Appl. Phys.* **76**, 7966 (1994).
5. A. Ketterson, F. Ponse, T. Henderson, J. Klem, H. Morkoc, *J. Appl. Phys.* **57**, 2305 (1985).
6. S.-J. Chua, S.H. Lee, *Jpn. J. Appl. Phys.* **33**, 66 (1994).
7. H.J. Bohlmann, M. Ilegems, *J. Electrochem. Soc.* **138**, 2795 (1991).
8. H. Goronkin, S. Tehrani, T. Rimmel, P.L. Fejes, K.J. Johnson, *IEEE Trans. Electron Devices.* **36**, 281 (1989).
9. T.S. Abhilash, Ch.R. Kumar, G. Rajaram, *J. Phys. D: Appl. Phys.* **42**, 125104 (2009).
10. H. H. Berger, *Solid State Electron.* **15**, 145 (1972).
11. C. Lin, C.P. Lee, *J. Appl. Phys.* **67**, 260 (1990).
12. T.S. Abhilash, Ch.R. Kumar, B. Sreedhar, G. Rajaram, *Semicond. Sci. Tech.* **25**, 035002 (2010).
13. T.S. Abhilash, Ch.R. Kumar, G. Rajaram, *Thin Solid Films* **518**, 5576 (2010).
14. T.S. Kuan, P.E. Batson, T.N. Jackson, H. Rupprecht, E.L. Wilkie, *J. Appl. Phys.* **54**, 6952 (1983).
15. M. Ogawa, *J. Appl. Phys.* **51**, 406 (1980).
16. M. Murakami, K.D. Childs, J.M. Baker, A. Callegari, *J. Vac. Sci. Technol. B* **4**, 903 (1986).
17. G.S. Saravanan, K.M. Bhat, K. Muraleedharan, H.P. Vyas, R. Muralidharan, A.P. Pathak, *Semicond. Sci. Tech.* **23**, 025019 (2008).
18. T. Kim, D.D.L. Chung, *Thin Solid Films* **147**, 177 (1987).